Asia-Pacific Journal of Science and Technology: Volume: 28. Issue: 03. Article ID.: APST-28-03-11. Research Article

APST

Asia-Pacific Journal of Science and Technology

https://www.tci-thaijo.org/index.php/APST/index

Published by the Research and Graduate Studies,
Khon Kaen University, Thailand

Preparation of activated carbon as supercapacitor electrode materials from cassava rhizome

Gittisak Phachwisoot[1,2], Chalathorn Chanthad[3], Kamonwat Nakason[1,2,*], Pongtanawat Khemthong[3], Saran Youngjan[3] and Bunyarit Panyapinyopol[1,2]

[1]Department of Sanitary Engineering, Faculty of Public Health, Mahidol University, Bangkok, Thailand
[2]Center of Excellence on Environmental Health and Toxicology (EHT), OPS, MHESI, Bangkok, Thailand
[3]National Nanotechnology Center (NANOTEC), National Science and Technology Development Agency (NSTDA), Pathum Thani, Thailand
[*]Corresponding author: kamonwat.nak@mahidol.ac.th

Received 1 April 2022
Revised 6 May 2022
Accepted 10 May 2022

Abstract

In this study, activated carbon (AC) was prepared from raw cassava rhizome (CR) and CR hydrochar which was derived from a hydrothermal carbonization process at 200°C for 1 h in 0.4 M of aqueous HCl. The chemical activation process was further conducted using a raw material to $ZnCl_2$ ratio of 1:3 at 800°C for 2 h under nitrogen atmosphere. Elemental compositions, graphitization degree, porosity, specific surface area (SSA), surface chemical functional groups and morphology of the AC were investigated. The analysis results demonstrated that the AC derived from raw CR (CRZ83) provided promising properties for using as supercapacitor electrode material (SEM). It had higher total pore volume (1.53 cm^3/g) and SSA (1,225 m^2/g) than those of the AC prepared from CR hydrochar (CRHZ83). Electrochemical potentials of the CRZ83 were investigated using a three-electrode system in 1 M H_2SO_4 electrolyte. Its specific capacitance was 123.0 F/g at a current density of 0.3 A/g. The results could suggest that the AC prepared from raw CR can be an alternative material for supercapacitor electrodes.

Keywords: Activated carbon, Hydrochar, Agricultural waste, Renewable energy, Energy storage, Biomass utilization

1. Introduction

The rapid expansion of the global economy has led to overexploitation of fossil-based energy sources, which has consequently resulted in resource depletion, environmental pollution and disease. Thus, novel alternative energy sources such as solar and wind have received huge attention [1]. To achieve maximum benefit, the energy derived from those eco-friendly energy sources has to be properly stored [2].

Supercapacitors have been regarded as a promising energy storage device. They have high power and energy densities, rapid charge-discharge capabilities, small size and long life cycles (more than 100,000 cycles) [3]. These features overcome many of the limitations of both conventional capacitors and batteries [4]. Supercapacitors generally consist of five major components including electrodes, separators, current collectors, conductive metal materials and leakage protectants [5]. The electrode is the most important part related to supercapacitor performance. In general, electrodes can be produced from various materials such as conductive polymers and metal oxides. The commercial use of these materials is limited because of their detrimental effect to human health and environment [6]. Therefore, discovering new materials is essential. Activated carbon (AC) is an eco-friendly and low cost material and has a high specific surface area (SSA) that is required to provide an adequate number of sites for charge accumulation on the electrode/electrolyte interface [7]. Thus, AC with high SSA is regarded as promising materials for supercapacitor electrode material (SEM). Normally, the AC for supercapacitor electrodes can be produced from various biomass wastes such as rice husk [8] and pineapple

leaves [9]. In the AC activation process, $ZnCl_2$, KOH, H_3PO_4 etc. are commonly employed as an activating agent. Among them, $ZnCl_2$ is regarded as an outstanding activating agent because of its mild properties, and high potential in porosity and SSA production [7].

Considering the potential biomass, cassava rhizome (CR) is the most promising candidate according to its plentiful biomass in Thailand. It constitutes a residue from the cassava harvest with the residue product ratio of CR is 0.2 [10]. CR is a connective joint between the cassava root and cassava stalk. In 2020, 29 million tons of cassava products were produced in Thailand, which is equivalent to the estimated amount of CR of 5.8 million tons [11]. CR is commonly disposed of by open burning at the plantation, resulting in substantial various environmental drawbacks, especially air pollution. Interestingly, CR contains high carbon content making it suitable for use as a feedstock in the production of AC for SEM [12]. On the other hand, CR use is restricted by its high moisture content [12,13]. Thus, to increase its use efficiency, a pretreatment process is required [12,13]. The process could stabilize raw biomass by removing volatile components through degradation reactions forming gas and tar [14,15]. Hydrothermal carbonization is an outstanding pretreatment technology for high moisture biomass [12]. It results in hydrochar as a substantial product which can be used as a feedstock for AC production. However, studies comparing between AC properties of SEM derived from raw CR and from CR hydrochar have never been conducted.

In this study, AC was prepared from raw CR and CR hydrochar via a chemical activation process using $ZnCl_2$ as an activating agent. The produced AC was characterized by elemental composition, graphitization degree, porosity, SSA, surface chemical functional groups and morphology. Electrochemical potentials of the promising AC were investigated using a three-electrode system in 1 M H_2SO_4 electrolyte.

2. Materials and methods

2.1 Materials

CR was used as a feedstock in this study and was collected to prepare CR powder using the method reported in a related study [16].

2.2 Preparation of AC

In this study, raw CR and CR hydrochar were used as a feedstock for preparing AC. The CR hydrochar was prepared using a catalytic hydrothermal carbonization process conducted in a batch autoclave reactor (250 mL, NK Laboratory Co., Ltd, Thailand). In the catalytic hydrothermal carbonization process, 18 g of the raw CR powder was mixed with 180 mL of 0.4 M aqueous HCl in a glass vessel which was inserted inside the reactor. Then the reactor was tightly closed and heated at 200°C for 1 h. For quenching reaction, the reactor was suddenly cooled to ambient temperature by placing in a water bath. The hydrochar was isolated from an aqueous phase by vacuum filtration.

The AC was produced through a chemical activation process [17-19]. In each experiment, 4 g of the feedstock was homogeneously mixed with 12 g of $ZnCl_2$ in a quartz boat, then placed in a horizontal tube furnace. Before heating, an inert environment in the tube furnace was initiated by purging nitrogen gas at 250 mL/min for 10 min. Then the sample was preheated at 105°C for 1 h and was further heated at 800°C with a ramping rate of 10°C/min for 2 h. After that, the temperature was physically dropped to ambient temperature. The product was first washed with 1 M aqueous HCl, and then washed with deionized water until the pH of the washed water became neutral [16]. The sample was dried at 105°C for 24 h. The AC derived from raw CR and CR hydrochar was designated as raw CR (CRZ83) and CR hydrochar (CRHZ83), respectively.

2.3 AC characterizations

The AC was characterized by elemental and proximate compositions, graphitization degree, porosity, SSA, surface functional groups and morphology, conducted according to the methods in the related study [16]. Elemental compositions were determined using an elemental analyzer (LECO CHNS 628). For proximate compositions, ash and volatile matter (VM) contents were determined through NREL/TP-510-42622 and American Society for Testing and Materials (ASTM) D 7582 methods, respectively. Fixed carbon (FC) content was determined by deducting 100% from ash and VM contents. Graphitization degree was measured using x-ray diffractometer (XRD), Bruker D8 ADVANCE) with Cu K_α radiation (λ = 1.5418 Å) and Raman spectra (High Resolution Raman, LabRAM HR Evolution) with a laser wavelength of 532 nm. Porosity and SSA were identified by physical adsorption of N_2 (NOVAe-Series surface area analyzer) at 77 K. Surface functional groups were determined by Fourier transform infrared spectroscopy (FT-IR, Thermo Fisher Scientific Nicolet 6700) using potassium bromide (KBr) pellet method in the range of 4000 to 400 cm^{-1}. Morphology was observed using field emission scanning electron microscopy (FE-SEM, JEOL JSM-7610F).

2.4 Fabrication of the electrodes and electrochemical measurements

The electrochemical potential of the electrode materials was investigated using a three-electrode system. The fabrication of supercapacitor electrodes and electrochemical measurements were conducted according to the steps of related studies [16]. The electrode was prepared by mixing the AC with a binder [polyvinylidene fluoride (PVDF)] and conductive carbon (Super P) with a weight ratio of 80:10:10 in an *N*-methyl-2-pyrrolidone (NMP) solvent, and then the mixture were coated on stainless-steel plates. The obtained electrode was dried in an oven at 80°C for 12 h and then dried in a vacuum oven at 80°C for 6 h. Pt and Ag/AgCl were used as counter and reference electrodes, and 1 M H_2SO_4 solution was used as the electrolyte for electrochemical tests. Specific capacitance of supercapacitor electrodes was calculated using Equation (1)

$$C = I \times \Delta t / m \times \Delta V \quad (1)$$

where C is the specific capacitance (F/g), I is the discharge current (A), Δt is the discharge time (s), m is the mass of AC (g), and ΔV is the voltage (V).

3. Results and discussion

3.1 Characterization of AC

Elemental compositions of raw CR, CRZ83 and CRHZ83 are tabulated in Table 1. As can be seen, carbon content of CRZ83 and CRHZ83 was much higher than raw CR, while oxygen and hydrogen contents of the AC were much lower than raw CR. Increasing carbon while decreasing oxygen and hydrogen contents were primary due to eliminating volatile components through the dehydration reaction of $ZnCl_2$ with heat treatment [14,17]. On the other hand, CRZ83 had higher carbon content but lower hydrogen and oxygen contents than that of CRHZ83. Interestingly, CRZ83 had lower ash and higher nitrogen contents than that of CRHZ83. Lower ash content could enhance SSA and pore volume of the material due to dense carbon. The nitrogen content could enhance the efficiency of the electrode materials because it improves the electrical conductivity in the storage mechanism of supercapacitor electrodes [20]. These results implied that CRZ83 could be a promising AC for being used as SEM.

Table 1 Elemental composition of raw CR, CRZ83, and CRHZ83.

Sample	Yield	Elemental composition (wt.%)					Proximate composition (wt.%)		
name	(dried wt.% on CR)	Carbon	Hydrogen	Nitrogen	Sulfur	Oxygen	Ash	VM	FC
CR	-	45.50	6.10	1.10	0.10	42.90	4.20	75.13	20.67
CRZ83	4.27	91.95	0.66	1.05	0.27	4.29	1.78	6.15	92.07
CRHZ83	8.51	90.26	0.77	0.83	0.20	4.63	3.30	4.92	90.45

Figure 1 depicts the graphitization degree of the AC through x-ray powder diffraction (XRD) (Figure 1A) and Raman spectra (Figure 1B). XRD spectra shows two dominant diffraction peaks at 24.1° and 43.1°, which are consistent with the (002) and (100) diffraction planes of the graphitic carbon, presenting that CRZ83 and CRHZ83 were made of both graphitic and amorphous structures [21]. On the other hand, the intensity peaks of CRZ83 were similar with that of CRHZ83, confirming that those graphitized structure degree did not differ much [22]. The graphitic structure of the AC was further confirmed through Raman spectra [23]. The two peaks at 1350 cm^{-1} and 1580 cm^{-1} appeared in the spectra corresponding to the D and G bands, respectively [24]. Typically, the D band represents the disordered carbonaceous structure, and the G band shows the graphitic structure. The intensity of the D and G bands are commonly used to determine charge-storage capacity and electrical conductivity of the materials [25]. The intensity ratio of the D to G bands (I_D/I_G) identifies the degree of the graphitic structure. A higher I_D/I_G ratio possesses lower degrees of graphitization and vice versa. The I_D/I_G value of CRZ83 and CRHZ83 were 0.88 and 0.90, respectively, indicating that the graphitic structure of CRZ83 was similar to CRHZ83. This result corresponds with the XRD spectra.

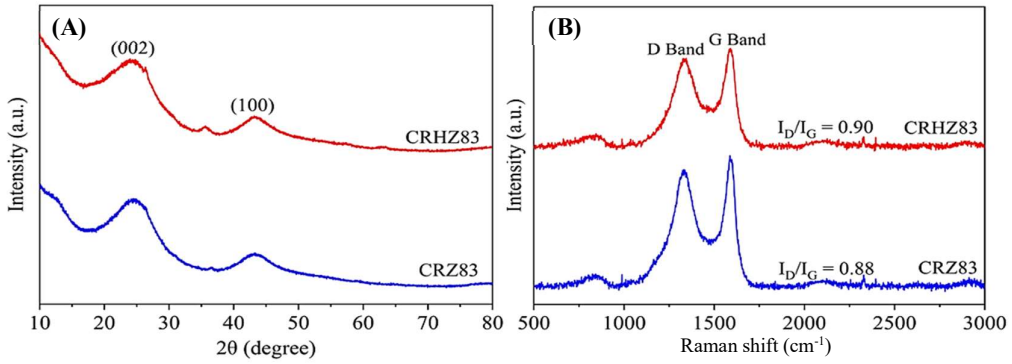

Figure 1 (A) XRD and (B) Raman spectra of CRZ83 and CRHZ83.

The SSA and pore properties of carbon materials substantially affected supercapacitor electrode performance. These characteristics are related to capacitance of the electrodes, because the SSA and pore properties are used to collect charge in an electrolyte by adsorption [26]. Due to $ZnCl_2$ activation, the nitrogen adsorption desorption isotherm in Figure 2A depicts that CRZ83 and CRHZ83 contain both micropores (<2 nm) and mesopores (2 to 50 nm) structures [16]. As already indicated, the full isotherms of both samples pronounced uptake at low P/P_0 and were associated hysteresis loops. The shapes of hysteresis loop of both samples were related to particular features of Type H4 attributed to the filling of micropore-mesopore. Both loops are initiated at $P/P_0 \sim 0.4$, but the CRHZ83 has a narrow branch and low adsorption volume compared with the CRZ83. As tabulated in Table 2, CRZ83 had an SSA and total pore volume of 1,225 m^2/g and 1.53 cm^3/g, respectively, which were higher than those of CRHZ83. SSA and total pore volume of CRHZ83 were 1,109 m^2/g and 0.91 cm^3/g, respectively. These results disagreed with the ash content of CRZ83 and CRHZ83. Figure 2B depicts that both CRZ83 and CRHZ83 contain average pore sizes of 3.71 nm and 3.72 nm, respectively, which is in the pore range relevant to supercapacitor properties [27]. These results determined that CRZ83 could be a promising AC for using as SEM.

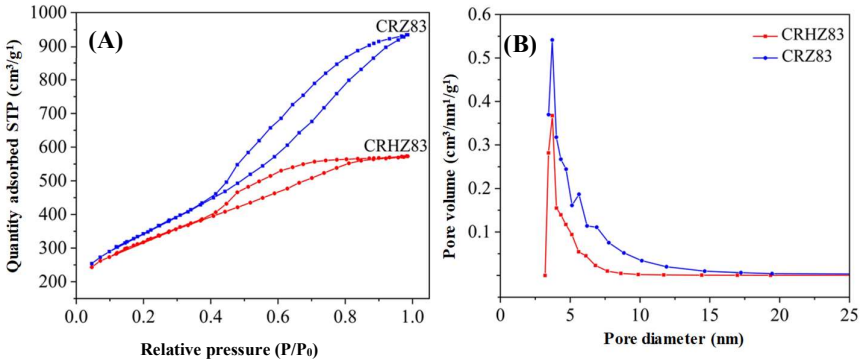

Figure 2 (A) N_2 adsorption desorption isotherms and (B) pore size distribution of CRZ83 and CRHZ83.

Table 2 SSA and pore properties of CRZ83 and CRHZ83.

Sample	S_{BET}[a] (m^2/g)	V_t[b] (cm^3/g)	V_{mi}[c] (cm^3/g)	V_{me}[d] (cm^3/g)	D_A[e] (nm)
CRZ83	1,225	1.53	0.35	1.18	3.71
CRHZ83	1,109	0.91	0.44	0.47	3.72

Note: [a] SSA, [b] Total pore volume, [c] Micropore volume, [d] Mesopore volume, [e] Average pore size.

The Fourier-transform infrared spectroscopy (FTIR) spectra in Figure 3 illustrate the surface functional groups of CR, CRZ83 and CRHZ83 samples. CR possessed five major peaks. The strong peak at the wavenumber of 3450 to 3500 cm^{-1} is ascribed to the O-H vibration from the hydroxyl group. The intensity of this peak in the CRZ83 and CRHZ83 was much lower than that of raw CR, corresponding with the changes of elemental compositions though the dehydration reaction [14,17]. The weak peak at 2850 to 2900 cm^{-1} is assigned to the C-H vibration from the aliphatic hydrocarbon which was preserved in the CRZ83 and CRHZ83 samples. The transmittance peak at 1650 cm^{-1} represented the C=O stretching vibration of ketone, amide and carboxylic groups [13]. This peak disappeared in CRZ83 and CRHZ83 samples because of the decarboxylation reaction. The peak at 1600 cm^{-1} is ascribed to the C=C vibration [28]. This peak of CRZ83 and CRHZ83

samples was shipped to 1589 cm^{-1} [28]. The peak at 1050 cm^{-1} corresponds to the C-O vibration of the carboxyl group which was shipped to 1147 cm^{-1} in [13,28]. The wave number changes of these peaks could be related to the activation reactions of $ZnCl_2$ at 800°C.

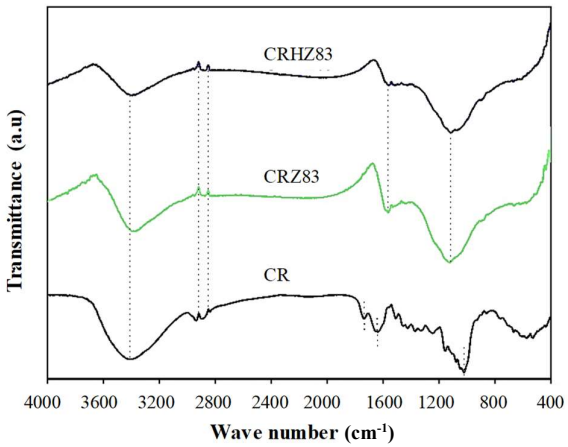

Figure 3 FT-IR spectrums of raw CR, CRZ83 and CRHZ83.

Surface morphology of raw CR, CRZ83 and CRHZ83 is illustrated in Figure 4. As can be seen, the morphology of raw CR (Figure 4A) was smooth and compact with small grooves. Because the raw CR was activated at 800°C with $ZnCl_2$ (Figure 4B and 4C), the surface became rough with numerous cavities. The surface of CRZ83 exhibited more roughness than that of CRHZ83 corresponding with higher SSA and pore properties in Table 2. CRZ83 showed an SSA and total pore volume of 1,225 m^2/g and 1.53 cm^3/g, respectively, which were higher than those of CRHZ83. SSA and total pore volume of CRHZ83 were 1,109 m^2/g and 0.91 cm^3/g, respectively.

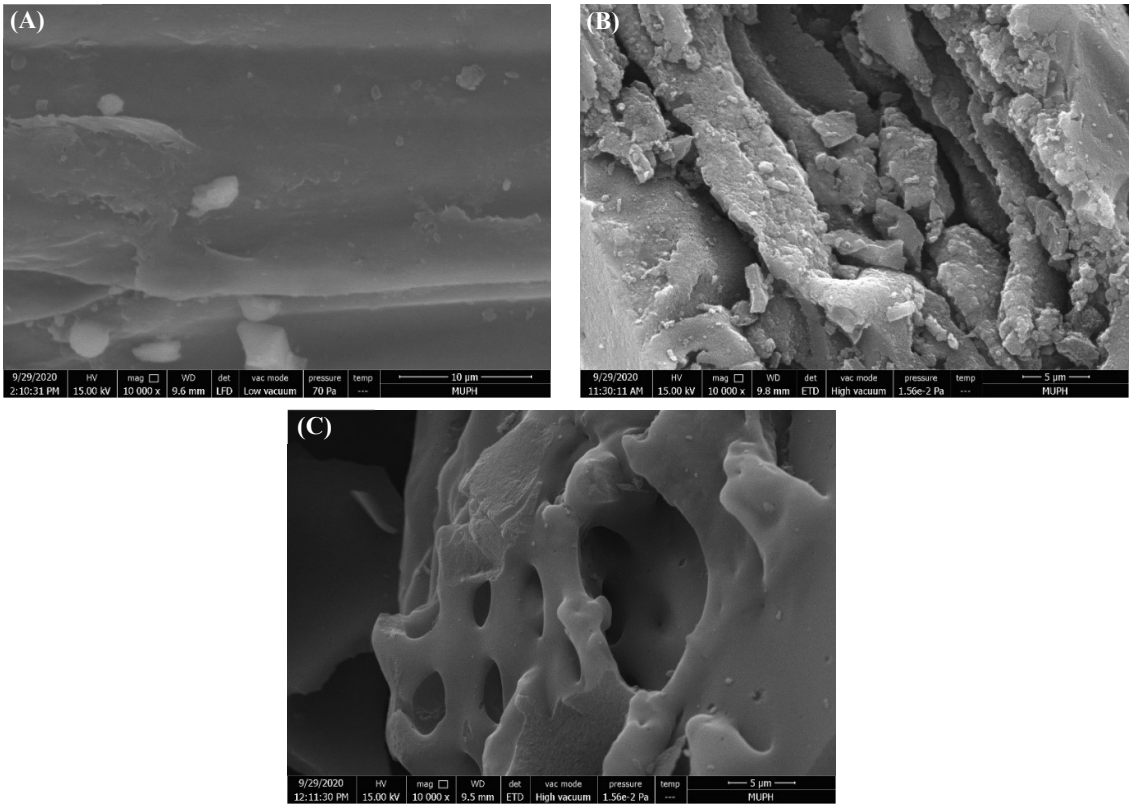

Figure 4 Surface morphology of raw: CR (A), CRZ83 (B), and CRHZ83 (C).

3.2 Electrochemical potential

The electrochemical potential of the electrode materials derived from CRZ83 was evaluated in 1 M H_2SO_4 for three-electrode systems. Figure 5A illustrates the CV curves of CRZ83 at scan rates and potential range of 10 to 100 mV/s and 0 to 1 V, respectively. As can be seen at a scan rate of 10 mV/s, the curve had an equally rectangular configuration without a redox peak, consistent with a property of an electrical double-layer capacitor (EDLC) [29]. The changes of scan rate affecting the redox peaks became broaden and distorted [30]. On the other hand, the changes of potential range affected the material resistance and irreversible reduction [31]. Galvanostatic charge-discharge (GCD) tests were conducted to measure the electrochemical capacitance of the sample. Figure 5B depicts the GCD curves in the potential range of 0 to 1 V at a current density of 0.3 A/g. The curve exhibited a nearly symmetric triangular shape, indicating promising capacitive characteristics and electrochemical reversibility of the material. The specific capacitance of the CRZ83 at a current density of 0.3 A/g was 123.0 F/g which was higher than that of dead ginkgo leaves (102 F/g) [32] and loofah sponge (107.4 F/g) [33].

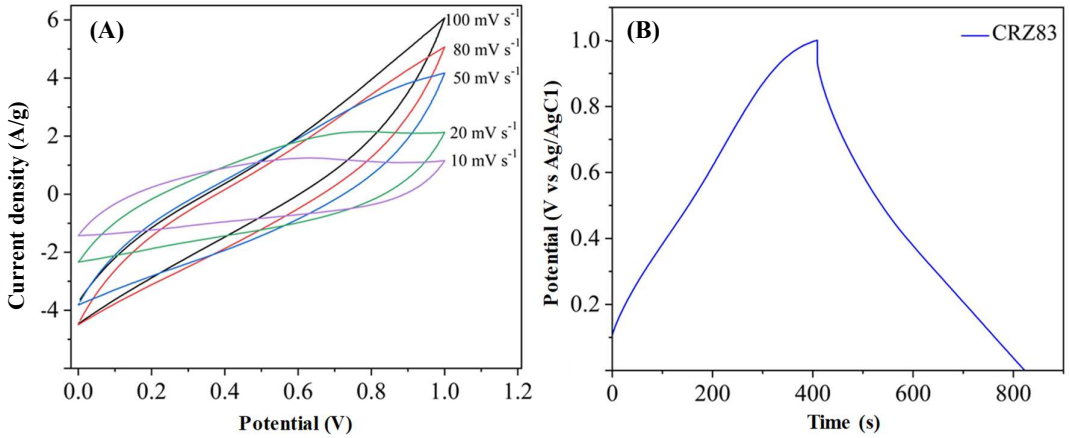

Figure 5 CV curve of CRZ83 at different scan rates (A) and GCD curve of CRZ83 at current density 0.3 A/g (B).

4. Conclusion

AC as SEM was prepared from raw CR and CR hydrochar through a chemical activation process using $ZnCl_2$ as an activating agent. The carbon derived from CRZ83 shows outstanding properties for use in SEM. It had higher nitrogen content, SSA, and pore volume than those of the carbon derived from CRHZ83. These results suggested that CR should not be pretreated before using as a feedstock to prepare AC as SEM. The specific capacitance of CRZ83 was 123.0 F/g at a current density of 0.3 A/g. Chemical doping should be further investigated to enhance the electrochemical potentials of CR and AC.

5. Acknowledgements

This project was funded by the National Research Council of Thailand (grant number: 195/2563) and partially supported by Mahidol University (grant number 114/2562) and National Nanotechnology Center (NANOTEC), National Science and Technology Development Agency (NSTDA), through grant number P1952435 and P1652028. The study was supported for publication by the China Medical Board (CMB), Faculty of Public Health, Mahidol University, Bangkok, Thailand. Financial assistance for this research was also provided by the Center of Excellent on Environmental Health and Toxicology (EHT), OPS, Ministry of Higher Education, Science, Research and Innovation.

6. References

[1] Khare V, Nema S, Baredar P. Solar-wind hybrid renewable energy system: a review. Renewable Sustainable Energy Rev. 2016;58:23-33.

[2] Cheng XB, Zhang R, Zhao CZ, Zhang Q. Toward safe lithium metal anode in rechargeable batteries: a review. Chem Rev. 2017;117(15):10403-10473.

[3] Zhang LL, Zhao XS. Carbon-based materials as supercapacitor electrodes. Chem Soc Rev. 2009;38(9):2520-2531.

[4] Yu K, Zhu H, Qi H, Liang C. High surface area carbon materials derived from corn stalk core as electrode for supercapacitor. Diamond Relat Mater. 2018;88:18-22.

[5] Stoller MD, Park S, Zhu Y, An J, Ruoff RS. Graphene-based ultracapacitors. Nano Lett. 2008;8(10):3498-3502.

[6] Carrell CJE, Li S, Parra AM, Shrestha B. 10 - metal oxide nanomaterials: health and environmental effects. In: Njuguna J, Pielichowski K, Zhu H, editors. Health and Environmental Safety of Nanomaterials.1st ed. Sawston: Woodhead Publishing; 2014. p. 200-221.

[7] Ahmed S, Ahmed A, Rafat M. Supercapacitor performance of activated carbon derived from rotten carrot in aqueous, organic and ionic liquid based electrolytes. J Saudi Chem Soc. 2018;22(8):993-1002.

[8] Liu D, Zhang W, Lin H, Li Y, Lu H, Wang Y. A green technology for the preparation of high capacitance rice husk-based activated carbon. J Cleaner Prod. 2016;112:1190-1198.

[9] Sodtipinta J, Amornsakchai T, Pakawatpanurut P. Nanoporous carbon derived from agro-waste pineapple leaves for supercapacitor electrode. Adv Nat Sci Nanosci Nanotechnol. 2017;8(3):035017.

[10] Department of Alternative Energy Development and Efficiency. Biomass potential in Thailand, http://biomass.dede.go.th/biomass_web/index.html [accessed 30 June 2021].

[11] Centre for Agricultural Information, Agricultural Production Data. Agricultural production data, http://www.oae.go.th/view/1/%E0%B8%82%E0%B9%89%E0%B8%AD%E0%B8%A1%E0%B8%B9%E0%B8%A5%E0%B8%81%E0%B8%B2%E0%B8%A3%E0%B8%9C%E0%B8%A5%E0%B8%B4%E0%B8%95%E0%B8%AA%E0%B8%B4%E0%B8%99%E0%B8%84%E0%B9%89%E0%B8%B2%E0%B9%80%E0%B8%81%E0%B8%A9%E0%B8%95%E0%B8%A3/TH-TH [accessed 30 June 2021].

[12] Nakason K, Panyapinyopol B, Kanokkantapong V, Viriya-empikul N, Kraithong W, Pavasant P. Characteristics of hydrochar and liquid fraction from hydrothermal carbonization of cassava rhizome. J Energy Inst. 2018;91(2):184-193.

[13] Nakason K, Khemthong P, Kraithong W, Chukaew P, Panyapinyopol B, Kitkaew D, et al. Upgrading properties of biochar fuel derived from cassava rhizome via torrefaction: effect of sweeping gas atmospheres and its economic feasibility. Case Stud. Therm. Eng. 2021;23:100823.

[14] Gao Z, Zhang Y, Song N, Li X. Biomass-derived renewable carbon materials for electrochemical energy storage. Mater Res Lett. 2017;5(2):69-88.

[15] Hulicova D, Yamashita J, Soneda Y, Hatori H, Kodama M. Supercapacitors prepared from melamine-based carbon. Chem Mater. 2005;17(5):1241-1247.

[16] Phachwisoot G, Nakason K, Chanthad C, Khemthong P, Kraithong W, Youngjan S, et al. Sequential production of levulinic acid and supercapacitor electrode materials from cassava rhizome through an integrated biorefinery process. ACS Sustainable Chem Eng. 2021;9(23):7824-7836.

[17] Sattayarut V, Chanthad C, Khemthong P, Kuboon S, Wanchaem T, Phonyiem M, et al. Preparation and electrochemical performance of nitrogen-enriched activated carbon derived from silkworm pupae waste. RSC Adv. 2019;9(18):9878-9886.

[18] Wang C, Wu D, Wang H, Gao Z, Xu F, Jiang K. Biomass derived nitrogen-doped hierarchical porous carbon sheets for supercapacitors with high performance. J Colloid Interface Sci. 2018;523:133-143.

[19] Phiri J, Dou J, Vuorinen T, Gane PAC, Maloney TC. Highly porous willow wood-derived activated carbon for high-performance supercapacitor electrodes. ACS Omega. 2019;4(19):18108-18117.

[20] Wang Y, Zhang M, Dai Y, Wang HQ, Zhang H, Wang Q, et al. Nitrogen and phosphorus co-doped silkworm-cocoon-based self-activated porous carbon for high performance supercapacitors. J Power Sources. 2019;438:227045.

[21] Wang D, Fang G, Xue T, Ma J, Geng G. A melt route for the synthesis of activated carbon derived from carton box for high performance symmetric supercapacitor applications. J Power Sources. 2016;307:401-409.

[22] Ma G, Yang Q, Sun K, Peng H, Ran F, Zhao X, et al. Nitrogen-doped porous carbon derived from biomass waste for high-performance supercapacitor. Bioresour Technol. 2015;197:137-142.

[23] Ma F, Ding S, Ren H, Liu Y. Sakura-based activated carbon preparation and its performance in supercapacitor applications. RSC Adv. 2019;9(5):2474-2483.

[24] Jiang X, Guo F, Jia X, Liang S, Peng K, Qian L. Synthesis of biomass-based porous graphitic carbon combining chemical treatment and hydrothermal carbonization as promising electrode materials for supercapacitors. Ionics. 2020;26(7):3655-3668.

[25] Ahmed S, Ahmed A, Rafat M. Nitrogen doped activated carbon from pea skin for high performance supercapacitor. Mater Res Express. 2018;5(4):045508.

[26] Winter M, Brodd RJ. What are Batteries, fuel cells, and supercapacitors? Chem Rev. 2004;104(10):4245-4270.

[27] Gor GY, Thommes M, Cychosz KA, Neimark AV. Quenched solid density functional theory method for characterization of mesoporous carbons by nitrogen adsorption. Carbon. 2012;50(4):1583-1590.
[28] Yaumi AL, Bakar MZA, Hameed BH. Melamine-nitrogenated mesoporous activated carbon derived from rice husk for carbon dioxide adsorption in fixed-bed. Energy. 2018;155:46-55.
[29] Enock TK, King'ondu CK, Pogrebnoi A, Jande YAC. Status of biomass derived carbon materials for supercapacitor application. Int J Electrochem. 2017;2017:6453420.
[30] Zhu H, Li Y, Song Y, Zhao G, Wu W, Zhou S, et al. Effects of cyclic voltammetric scan rates, scan time, temperatures and carbon addition on sulphation of Pb disc electrodes in aqueous H_2SO_4. Mater Technol. 2020;35(3):135-140.
[31] Kozarenko OA, Dyadyun VS, Papakin MS, Posudievsky OY, Koshechko VG, Pokhodenko VD. Effect of potential range on electrochemical performance of polyaniline as a component of lithium battery electrodes. Electrochimica Acta. 2015;184:111-116.
[32] Zhu X, Yu S, Xu K, Zhang Y, Zhang L, Lou G, et al. Sustainable activated carbons from dead ginkgo leaves for supercapacitor electrode active materials. Chem Eng Sci. 2018;181:36-45.
[33] Li Z, Zhai K, Wang G, Li Q, Guo P. Preparation and electrocapacitive properties of hierarchical porous carbons based on loofah sponge. Materials. 2016;9(11):912.